

Biotechnological Communication

Synthesis, Characterisation and Antimicrobial Potential of Novel N-Alkylated Pyrrole Derivatives of Chitosan

Kalpana. P. R^{*1}, Rajasree R.² and Gurudayal Y¹¹Department of Pharmacy, Galgotias University, Greater Noida, Uttar Pradesh, India²School of Pharmacy, Amrita Vishwavidyapeetham, Edapally, Ernakulam, Kerala, India

ABSTRACT

Chitosan, a cationic biopolymer is a major derivative of chitin. It is biocompatible, non-toxic and environ-friendly material and has broad spectrum antimicrobial activity. However, it is less effective in neutral or basic conditions due to its solubility only in acidic medium. Therefore, chemical modification with suitable groups is necessary to enhance the potency of chitosan. The present study was mainly conducted to explore the effect of structural modifications on antimicrobial potential of chitosan. N-Methyl, N-Ethyl and N-Propyl pyrrole were reacted with N-chloroacyl-6-O-triphenylmethylchitosan prepared by stepwise modification of chitosan to form N-Methyl, N-Ethyl and N-Propyl pyrrole derivatives of chitosan. Structural characterization of these pyrrole derivatives was done by IR, NMR, XRD, DSC and Elemental Analysis. The gram-negative bacterium *Escherichia coli*, gram-positive bacterium *Staphylococcus aureus* were selected for antibacterial activity and the fungus *C. albicans* was selected for antifungal activity by agar diffusion method and MIC method. Antimicrobial activity of the N-Methyl, N-Ethyl and N-Propyl pyrrole derivatives on *E. coli*, *S. aureus* and *C. albicans* showed an inhibitory effect on all the organisms. The potency of inhibition was found to be varied with the substitutions. The maximum activity was shown by N-pyrrolylpropylchitosan against *E. coli* (zone of inhibition 1.2±0.05cm, MIC 0.15±0.03mg/ml), *S. aureus* (zone of inhibition 1.4±0.03cm, MIC 0.15±0.01mg/ml), *C. albicans* (zone of inhibition 0.8±0.03cm, MIC 0.2±0.03mg/ml). The study also confirmed that all the three derivatives exhibited higher inhibition than that of chitosan against *E. coli* (zone of inhibition 0.7±0.03cm, MIC 0.09±0.02mg/ml), *S. aureus* (zone of inhibition 0.8±0.03cm, MIC 0.09±0.02mg/ml), *C. albicans* (zone of inhibition 0.6±0.03cm, MIC 0.09±0.03mg/ml). Results demonstrated that these three N-alkylpyrrole chitosan derivatives exhibited improved potency and hence can have the more applicability as antimicrobials..

KEY WORDS: ANTIMICROBIAL ACTIVITY, CHITOSAN, CHARACTERIZATION, N-CHLOROACYL-6-O-TRIPHENYLMETHYLCHITOSAN, STRUCTURAL MODIFICATION.

INTRODUCTION

Chitosan, a linear heteropolymer is now considered as a functional biopolymer. It is widely exploited for its applications on account of its biodegradability, biocompatibility, versatility and also is found plentiful in nature (Mati-Bauche et al. 2014). Chitosan is the major derivative of the chitin. It is readily soluble in diluted acetic acid (Kumari et al. 2017). Chitosan gained curiosity of researchers not only because of its various properties but also due to its unique biological applications such as antimicrobial, hypocholesterolemic, antitumor, anti-inflammatory, antioxidant, angiotensin-I-converting enzyme (ACE) inhibition, excluding toxins from the intestines, reducing heavy-metal poisoning in humans, mucoadhesive

haemostatic, analgesic, radio-protective properties, preventing tooth decay and tooth diseases and immunity enhancing activities (Chien et al. 2016; Prąglowska et al. 2019). It is also widely used in biomedical industries for enzyme immobilization and purification, in chemical plants for wastewater treatment and in food industries for food formulations as binding, gelling, thickening and stabilizing agent (Hosseinnejad et al. 2016; Nadia et al. 2019; Adnan et al. 2020).

Chemical modification of chitosan has thus provided a new way for developing more and more new derivatives having promising biological activities and physicochemical properties. Chitosan has a primary amino group (C2), and a primary and secondary free hydroxyl group (C3, C6) and this strong functionality of chitosan (per-repeat unit) gives it a considerable chance of chemical modification (Aranaz et al. 2010; Adnan et al. 2020). Pyrrole containing heterocyclic derivatives has been reported for exhibiting wide biological

Article Information:*Corresponding Author: rahatekalpana@gmail.com

Received 25/10/2021 Accepted after revision 26/12/2021

Published: 31st December 2021 Pp- 1730-1736

This is an open access article under Creative Commons License,

Published by Society for Science & Nature, Bhopal India.

Available at: <https://bbrc.in/> DOI: <http://dx.doi.org/10.21786/bbrc/14.4.52>

applications, like antibacterial, antioxidant, cytotoxic, insecticidal, anti-inflammatory, anticoagulant, antiallergic, antiarrhythmic, hypotensive and anticonvulsant, due to which they are preferred in a variety of medicinal agents (Parmar et al. 2012; Masci et al. 2019; Kundu and Pramanik 2020).

Due to limited solubility chitosan has not been an effective antimicrobial agent. Thus, in order to enhance the solubility and to broaden antimicrobial activity of chitosan, present study was taken up to synthesize N-alkylated pyrrole derivatives of chitosan and to compare their antibacterial and antifungal property with chitosan.

MATERIAL AND METHODS

Chitosan (CS) was purchased from Nitte gelatin India Limited (Kochi, Kerala, degree of deacetylation 76%). All the other chemicals were purchased from Loba Chemie, Sisco research laboratories, Spectrum Reagents and Chemicals, Alfa Aesar, Nice Chemicals. All the chemicals were used without any further purification. Synthesis of N-Chloroacetyl-6-O-triphenylmethyl chitosan intermediate from chitosan (Fig. 1) was done as per the procedure reported earlier. N-Chloroacetyl-6-O-triphenylmethyl chitosan intermediate was synthesized stepwise from Chitosan. It (10g) was dispersed overnight in DMF (200 mL), treated with Phthalic anhydride (27.6 g, 186 mmol) at 120°C for 8 h to obtain N-Phthaloylchitosan.

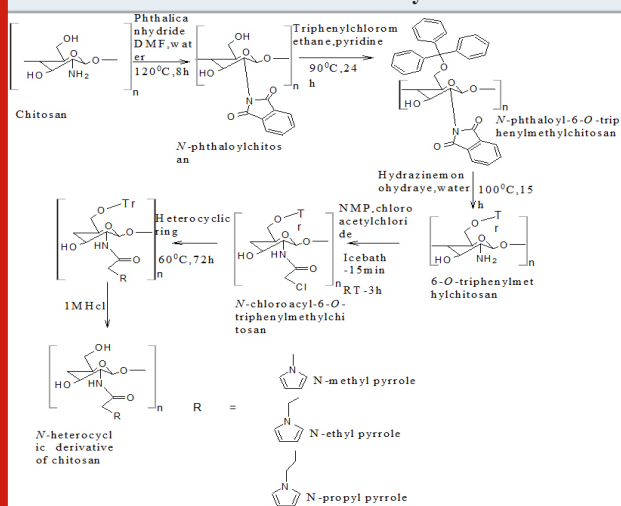
Triphenyl chloromethane (43.8 g, 157.2 mmol) was then added to a solution N-phthaloylchitosan (14.31 g, 52.45 mmol) in pyridine (215 mL) and stirred at 90°C for 24 h to form N-Phthaloyl-6-O-triphenylmethylchitosan. Upon reaction with hydrazine monohydrate (148 mL, 3.04 mol) at 100°C for 15 h, N-Phthaloyl-6-O-triphenylmethylchitosan (26.37 g, 45.06 mmol) was then converted into 6-O-Triphenylmethylchitosan, which was then acetylated by dropwise addition of chloroacetyl chloride to form N-Chloroacetyl-6-O-triphenylmethylchitosan intermediate (Holappa et al. 2005).

The N-alkylated pyrrole derivatives of chitosan (NPCS) were prepared by treating N-chloroacetyl-6-O-triphenylmethyl chitosan intermediate with the corresponding N-alkylated heterocyclic derivatives. N-Chloroacetyl-6-O-triphenylmethyl chitosan was stirred in N-methyl, N-ethyl, N-propyl pyrrole (25mg/mL) separately at 60°C for 72 h under argon. Results are mentioned in figure 1. The corresponding alkylated derivatives were evaporated from the reaction mixtures and washed with methanol and diethyl ether and dried in hot air oven at 80°C for 5 h and melting point was determined by using capillary melting point apparatus (Ma et al. 2008). Percent yield was computed by the following equation: Percent yield = Degree of substitution x (Molecular weight of starting material – Molecular weight of product / Molecular weight of starting material) x 100. Degree of substitution can be obtained from elemental analysis.

For the study of physicochemical properties, the intrinsic viscosity of CS and NPCS was measured by Ostwald viscometer. Mixture of 0.1 M acetic acid and of 0.2 M

sodium chloride solution (1:2) was used as solvent. The solutions were filtered through a filter paper to remove insoluble impurities and then were passed through the viscometer. Intrinsic viscosity ($[\eta]$) was calculated. The molecular weight of chitosan and NPCS was determined by Staudinger equation $\log [\eta] = \log K + a \log M_v$,

Figure 1: Synthetic route for novel N-alkylated pyrrole derivatives of chitosan via N-chloroacetylation



where, K and a are constant values: $1.8 \cdot 10^{-3}$ and 0.93 respectively (Lallana et al. 2017).

For the determination of swelling index, swelling capacity of the CS and NPCS was studied in different media. Previously weighed derivative samples (0.5 g for each test) were individually immersed in 30 mL 0.1 M acetic acid, Phosphate buffer saline of pH 7.4, distilled water and 0.1 M NaOH. The samples were then recovered from the media when they reached equilibrium swelling (24h), wiped with filter paper and weighed. The swelling ratio of each sample was determined according to the following equation: Swelling ratio (%) = $(W_t - W_o) / W_o \times 100$.

For characterisation, Fourier transform infrared (FT-IR) spectra of NPCS were measured in the 4000–400 cm^{-1} regions using a Thermo Nicolet Avatar 370 FT-IR spectrometer in KBr discs. Solid state ^{13}C and ^1H NMR spectra were recorded from a Bruker spectropin-400MHz spectrometer. The percentage elemental analysis (C, H, N and S) was performed on Elementar Vario EL III analyser. XRD measurement of the powder samples were performed with a D8 advance diffractometer (Bruker) with $\text{CuK}\alpha$ radiation ($\lambda = 0.154 \text{ nm}$, 40 kV, 100 mA, scanning rate 40/min). DSC temperature scan was performed on Mettler Toledo DSC 822e (temperature rate $10^\circ/\text{min}$). The degree of substitution was calculated by using the values of C/N ratio obtained from the elemental analysis (Shang et al. 2011; Jiao et al. 2011; Wang et al. 2021).

The antimicrobial activity of chitosan (CS) and NPCS was examined against Gram-positive (*Staphylococcus aureus*) and Gram-negative (*Escherichia coli*) bacterial and fungal strain (*Candida albicans*) by Agar diffusion

method and Minimum Inhibitory Concentration (MIC) method. Ciprofloxacin and Ketoconazole (0.25 mg) were used as standards respectively. Preliminary screening tests were performed at concentrations ranging from 0.1 to 3.0 mg/ml. Nutrient agar was used as culture media for antibacterial studies and Sabouraud dextrose agar was used for antifungal study (Hamid et al. 2011; Gharieb et

al. 2015). MIC was recorded in each case as the minimum concentration of compound which inhibited the growth of tested microorganism after incubation at 37°C for 24 h. From the MIC observed, the intermediate concentrations between MIC values were prepared by suitable dilution of stock solution to determine accurate MIC values. Each concentration was tested in triplicate (Li and Zhuang 2020; Lo et al. 2020).

Table 1. Percent Yield (%), M.P. (°C), viscosity [η], and swelling index (%) of chitosan and N-alkylated pyrrole derivatives of chitosan

Sample	% Yield	M. P. (°C)	Intrinsic Viscosity [η]	Swelling ratio %		
				0.1M NaOH	Phosphate buffer	0.1M CH ₃ COOH
CS	-	-	1154	60	54	58
S1	57	233-236	2868	64	78	80
S2	38	245-251	8578	66	70	78
S3	31	285-288	9855	70	84	94

Table 2. Elemental composition and degree of substitution of chitosan and N-alkylated pyrrole derivatives of chitosan

Sample	Theoretical values			Experimental values			C/N Ratio	Degree of substitution (DS)
	C	N	H	C	N	H		
CS	43.52	7.25	7.83	40.34	7.14	7.25	5.6	-
S1	57.68	4.97	5.74	55.73	4.33	5.30	12.8	1.02
S2	58.88	6.58	8.03	57.18	4.93	7.97	11.6	0.75
S3	62.98	6.23	8.29	61.18	5.16	8.02	11.8	0.69

RESULTS AND DISCUSSION

Yield and Physicochemical properties: The yield of N-methylpyrrole derivative of chitosan was found to be highest as compared with N-ethylpyrrole and N-propylpyrrole derivatives. It was found that after the chemical modification there was increase in intrinsic viscosity [η] of the resultant derivatives. There has been significant increase in the swelling index of NPCS compared to that of CS. The results are mentioned in table 1. The improved swelling index due to increase in rate of hydration indicated for better absorption of the drug.

Elemental analysis: After elemental analysis of CS and N-methyl, N-ethyl and N-propylpyrrole derivatives (S1, S2, S3) the values of percent of carbon, hydrogen and nitrogen were found experimentally close to the values obtained theoretically (Jauris et al. 2017). The C/N ratios were also calculated and from that the degree of substitution (DS) was determined. The values of DS suggested full N substitution in all the NPCS (Barbosa et al. 2019). The results are shown in table 2.

X-Ray Diffraction (XRD) analysis: XRD diffractogram of CS showed the characteristic peaks at 10.3° and 20.1°, which suggested the formation of inter and intra-molecular

hydrogen bonds in the presence of free amino groups. Absence of these two peaks in the spectra of all three NPCS confirmed that CS was substituted by the corresponding substituents added. In the samples S1 peak at 4.5° was attributed to the alkyl chain and the other two peaks at 26.6° and 15.5° were formed for pyrrole moiety. S2 showed two peaks at 4.30 and 4.5° for alkyl chain and two peaks at 25.7° and 15.80 for the pyrrole moiety and in S3 the peaks at 4.3° and 5.5° attributed to the alkyl chain and the peaks at 25.6° and 14.6° for the pyrrole nucleus chitosan (Mobarak et al. 2010; Wang et al. 2014; Pati et al. 2020). The crystalline index of CS as well as PCS was determined by following formula:

$$\text{Crystalline index (\%)} = \frac{(I_{110} - I_{am})}{I_{110}} \times 100$$

Where, I_{110} is the maximum intensity approximate to 200 and I_{am} is the intensity approximate to 160 (Cheng et al. 2020).

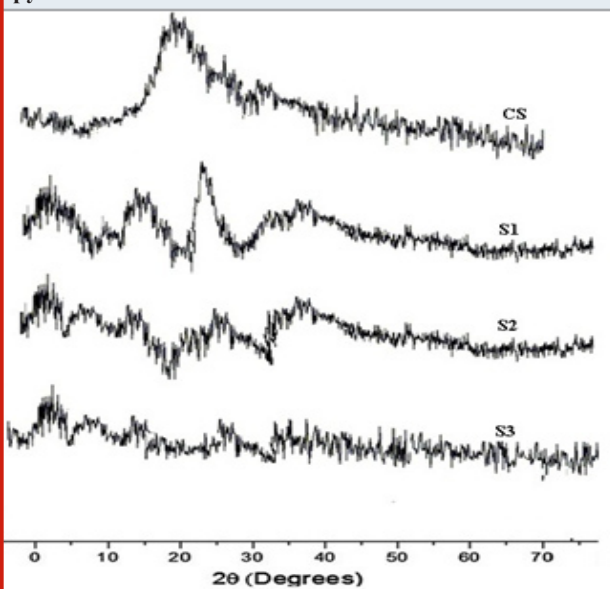
From the XRD results it was observed that the crystallinity of NPCS changed reasonably from that of CS. It is observed that S1, S2 and S3 showed crystalline index comparable to that of CS. It is also seen that S3 showed more crystalline

index than S1 and S2. The crystallinity index of CS and NPCS were shown in table 5. The diffractograms of CS and PCS were shown in figure 2.

Table 3. Crystalline index of chitosan and N-alkylated pyrrole derivatives of chitosan

Samples	Crystalline index (%)
CS	48
S1	41
S2	38
S3	42

Figure 2: XRD diffractogram of chitosan and N-alkylated pyrrole derivatives of chitosan



DSC analysis: Thermogram of CS showed typical polysaccharide behaviour with two distinct degradation stages. The first wide peak started at 30°C and continued up to 150°C, which corresponding to a dehydration process. The second stage started at 245°C and an elevation in the baseline, corresponding to combustion of the sample, was observed. No exothermic melting peak was displayed due to the amorphous state of the CS. Main melting point of chitosan was attributed to the peak which started from 245°C. This coincided with the melting point found out from the capillary melting point apparatus. Thermogram of CS was presented in figure 3a. The thermogram of S1 showed three distinct peaks of which two peaks corresponded to the degradation endothermic peak and the third one for the exothermic peak. The results were exhibited in figure 3b (Alipour et al. 2019; Ferreira et al. 2020).

From the DSC values it could be concluded that the peak at 95.59°C corresponded to dehydration of the sample. The second peak at 163.52°C corresponded to the melting of sample. The third stage showed a positive peak which was exothermic in nature which was due to the curing of the sample. The peak at 163.52°C clearly coincided with

the melting point found out from the capillary melting point apparatus. Thermogram of S2 showed two distinct endothermic peaks at 118.98°C and 218.98°C which showed the degradation as well as the melting of sample. The melting point of S2 obtained from DSC agreed with the value obtained by capillary melting point apparatus. S3 showed two endothermic peaks at 76.55°C and 112.75°C which corresponded to the loss of water and the melting of the sample. The sample showed similar melting points for both DSC as well as capillary tube method. The DSC result coincided with the results of XRD in such a way that the chitosan as well as the derivatives were weakly crystalline (Alipour et al. 2019; Ferreira et al. 2020).

Figure 3a: Thermogram of chitosan

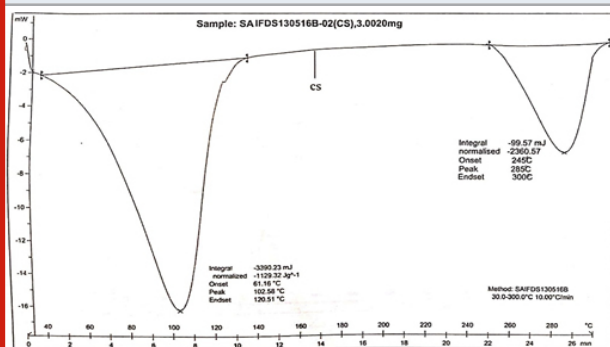
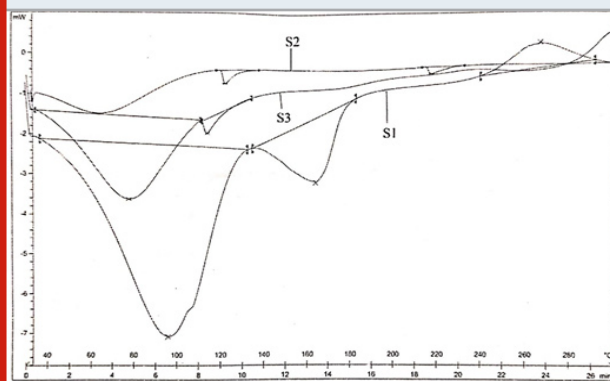


Figure 3b: Thermograms of N-alkylated pyrrole derivatives of chitosan

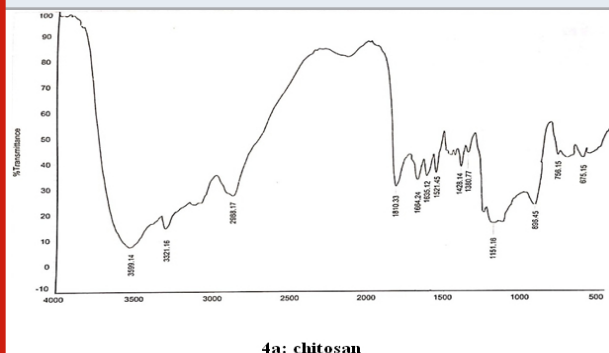


Spectral data of chitosan (CS): FT-IR: 3587 (O-H stretching), 3498 (N-H stretching), 2924 (N-H bond in CH₂), 2881 (C-H bond in CH₃), 1680 (N-H deformations of amide I), 1589 (Amide II), 1378 (CH₃ symmetrical deformation), 1080 (C-O-C bonds), 1421 (Methyl), 1153 (Asymmetric vibration of C-O in oxygen bridge), 896 (Wagging of saccharide structure of chitosan), 645 (C-H bend in aromatics). ¹³CNMR: δ (98.32, 56.95, 70.92, 78.07, 75.74, 61.43). ¹H NMR: 2.09–2.12 (s, NHCOCH₃), 3.15–3.30 (m, H-2 of GlcN residue), 3.57–4.10 (m, H-3,4,5,6 of GlcN unit and H- 2,3,4,5,6 of GlcNAc unit) and 4.88–5.00 (m, H-1 of GlcN and GlcNAc units). Spectra of chitosan coincided with that reported earlier (Verlee et al. 2017; Haj et al. 2020; Lal et al. 2020).

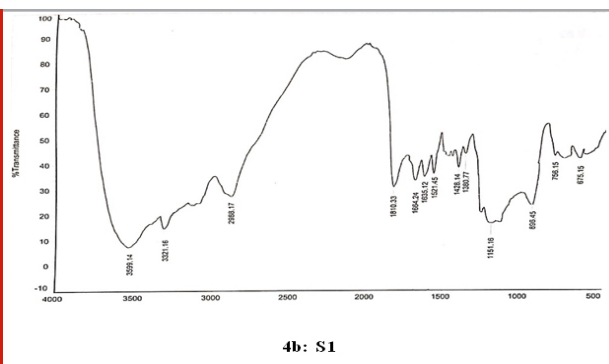
Spectral data of N-pyrrolylmethyl chitosan (S1): FT-IR: 3599 (O-H stretching), 3320 (N-H stretching), 2988 (C-H

stretching in CH₂), 1810 (C=O stretching), 1665 (Amide I), 1630 (C=C stretching in ring), 1519 (Amide II), 1429 (C=N stretching in ring), 1380 (C-N stretching), 1150 (Assymmetric vibration of C-O in oxygen bridge), 896 (Wagging of saccharide structure of chitosan), 747 (C-H bend mono in aromatics), 675 (C-H bend mono in aromatics). ¹³C NMR δ (98.33, 56.98, 70.91, 78.08, 75.45, 62.44, 178.09, 23.12, 109.22, 121.58, 35.82). ¹H NMR: 1.824 (s, 1H), 3.338 (s, 1H), 3.57–4.10 (m, H-3,4,5,6 of GlcN unit and H-2,3,4,5,6 of GlcNAc unit), 3.626 (s, 3H), 4.519 (s, 2H), 4.896 (d, J=2.4, 1H), 6.128 (s, 2H), 6.638 (s, 2H).

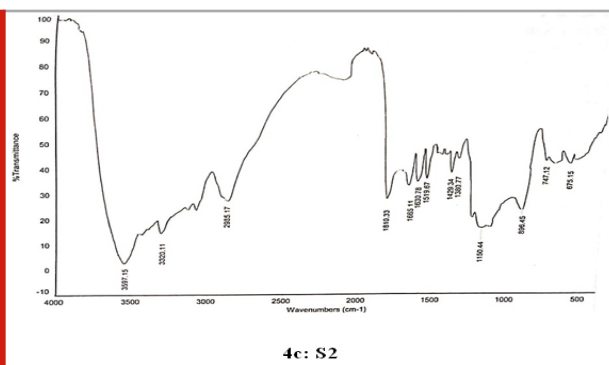
Figure 4: Infrared spectra of chitosan and N-alkylated pyrrole derivatives (S1,S2,S3) of chitosan



4a: chitosan

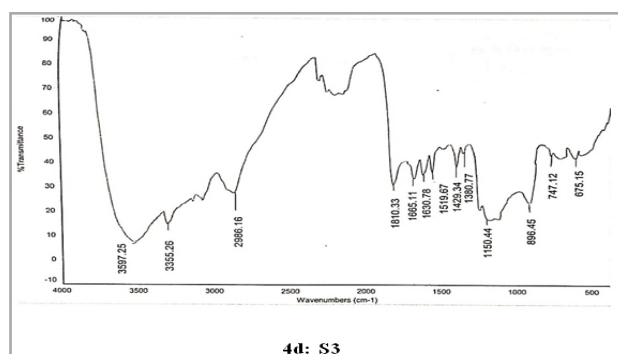


4b: S1



4c: S2

Spectral data of N-pyrrolylethyl chitosan (S2): FT-IR: 3597 (O-H stretching), 3335 (N-H stretching), 2986 (C-H stretching in CH₂), 1810 (C=O stretching), 1665 (Amide I), 1630 (C=C stretching in ring), 1519 (Amide II), 1429 (C=N stretching in ring), 1380 (C-N stretching), 1150 (Assymmetric vibration of C-O in oxygen bridge), 896 (Wagging of saccharide structure of chitosan), 747 (C-H bend mono in aromatics), 675 (C-H bend mono in aromatics). ¹³C NMR:



4d: S3

δ (99.53, 57.98, 71.99, 78.21, 75.77, 62.45, 179.81, 22.33, 109.05, 121.19, 44.68, 16.89). ¹H NMR: 1.391 (s, 2H), 1.823 (s, 1H), 3.331 (s, 1H), 3.57–4.10 (m, H-3,4,5,6 of GlcN unit and H-2,3,4,5,6 of GlcNAc unit), 3.670 (s, 3H), 4.356 (s, 2H), 4.519 (s, 2H), 4.897 (d, J=1.6, 1H), 6.221 (s, 2H), 6.964 (s, 2H).

Spectral data of N-pyrrolylpropyl chitosan (S3): FT-IR: 3589 (O-H stretching), 3355 (N-H stretching), 2986 (C-H stretching in CH₂), 1810 (C=O stretching), 1665 (Amide I), 1630 (C=C stretching in ring), 1519 (Amide II), 1429 (C=N stretching in ring), 1380 (C-N stretching), 1150 (Assymmetric vibration of C-O in oxygen bridge), 896 (Wagging of saccharide structure of chitosan), 747 (C-H bend mono in aromatics), 675 (C-H bend mono in aromatics). ¹³C NMR: δ (98.32, 55.98, 70.91, 78.08, 75.76, 62.43, 178.58, 22.12, 108.10, 122.18, 45.66, 16.88, 10.67). ¹H NMR: 1.362 (s, 2H), 1.824 (s, 1H), 1.893 (s, 2H), 2.101 (s, 2H), 3.332 (s, 1H), 3.57–4.10 (m, H-3,4,5,6 of GlcN unit and H-2,3,4,5,6 of GlcNAc unit), 3.678 (s, 3H), 4.515 (s, 2H), 4.895 (d, J=1.6, 1H), 6.216 (s, 2H), 6.362 (s, 2H), 6.965 (s, 2H).

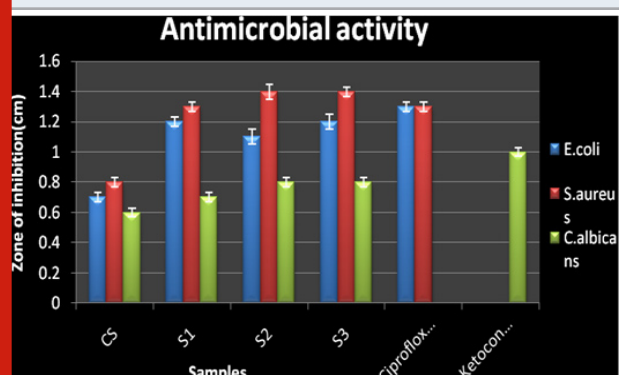
Antimicrobial activity: Chitosan and the three N-alkylated pyrrole derivatives of chitosan S1, S2, and S3 were screened for antimicrobial activity at different concentrations 2 μl, 5 μl, 10 μl, 15 μl, 20 μl, and 25 μl against *E. coli*, *S. aureus* and *C. albicans* by Agar diffusion assay method. The antimicrobial results of the chitosan derivatives against the bacteria and fungi were shown in table 6.

In general, NPCS showed significant antibacterial as well as antifungal activity against the bacteria *E. coli* and *S. aureus* and fungi *C. albicans* than native CS against *E. coli* (zone of inhibition 0.7±0.03 cm, MIC 0.09 mg/ml), *S. aureus* (zone of inhibition 0.8±0.03 cm, MIC 0.09 mg/mL) and *C. albicans* (zone of inhibition 0.6±0.03 cm, MIC 0.09 mg/mL). The maximum activity was shown by N-pyrrolylpropyl chitosan against *E. coli* (zone of inhibition 1.2±0.05 cm, MIC 0.15±0.03 mg/mL), *S. aureus* (zone of inhibition 1.4±0.03 cm, MIC 0.15±0.01 mg/mL), *C. albicans* (zone of inhibition 0.8±0.03 cm, MIC 0.2±0.03 mg/mL). From the results it was also a relevant fact that as the number of alkyl group increased the antimicrobial activity was also seen to be increasing as reported earlier (Panzariu et al. 2016; Mahira et al. 2019). Thus, it was concluded that antimicrobial activity of chitosan was enhanced obviously via chemical modification. The introduction of the substituent group at C-2 position increased the antimicrobial activity of CS.

Table 4. Antimicrobial activity of chitosan and N-alkylated pyrrole derivatives of chitosan by agar diffusion and MIC method

Sample	zone of inhibition (cm)			*Minimum Inhibitory Concn (mg/ml)*		
	<i>E.coli</i>	<i>S. aureus</i>	<i>C. albicans</i>	* <i>E. coli</i>	* <i>S. aureus</i>	* <i>C. albicans</i>
CS	0.7±0.03	0.8±0.03	0.6±0.03	0.09±0.02	0.09±0.02	0.09±0.03
S1	1.2±0.03	1.3±0.03	0.7±0.03	0.15±0.03	0.15±0.02	0.2±0.02
S2	1.1±0.05	1.4±0.05	0.8±0.03	0.15±0.02	0.15±0.02	0.2±0.03
S3	1.2±0.05	1.4±0.03	0.8±0.03	0.15±0.03	0.15±0.01	0.2±0.03
Ciprofloxacin	1.3	1.3	-	-	-	-
Keroconazole	-	-	1	-	-	-

* Values mean±SD mentioned for n=3.

Figure 5: Antimicrobial activity of chitosan and N-alkylated pyrrole derivatives of chitosan

CONCLUSION

The findings of the present study determine the antimicrobial activity that showed an improved antibacterial and antifungal activity as compared to chitosan. The activity of the N-propylpyrrole chitosan was maximum and comparable to that of the standards suggested that with increase in alkyl chain length the solubility and hence antimicrobial activity of the synthesized compounds also increased. The results may play a significant role in designing more potent chitosan derivatives. For this study, three novel N-alkylpyrrole derivatives of chitosan were synthesized by substitution on the reactive amino group of chitosan and characterized by FTIR and NMR spectral study. The compounds had low crystallinity and thermal stability comparable to chitosan.

ACKNOWLEDGEMENTS

The laboratory facilities for this study were provided by the Amrita School of Pharmacy, Amrita Vishwavidyapeetham, Kerala, India.

Conflict of Interests: Authors declare no conflict of interests to disclose.

REFERENCES

Adnan S, Ranjha NM, Hanif M et al. (2020).

O-Carboxymethylated chitosan; A promising tool with *in-vivo* anti-inflammatory and analgesic properties in albino rats. International Journal of Biological Macromolecules, Vol 156 pp 531-536.

Alipour M, Bigdeli MR, Aligholi H, et al. (2019). Sustained release of silibinin-loaded chitosan nanoparticle induced apoptosis in glioma cells. BioMed Research International, Vol 108 No 3 pp 458-469.

Aranaz I, Harris R, and Heras A (2010). Chitosan amphiphilic derivatives. Chemistry and applications. Current Organic Chemistry, Vol 14 No 3 pp 308-330.

Barbosa RFS, Souza AG, Ferreira FF, et al. (2019). Isolation and acetylation of cellulose nanostructures with a homogeneous system. Carbohydrate Polymers, Vol 218 pp 208-217.

Baskar D and Kumar TS (2009). Effect of deacetylation time on the preparation, properties and swelling behavior of chitosan films. Carbohydrate Polymers, Vol 78 No 4 pp 767-772.

Chien R, Yen M and Mau J (2016). Antimicrobial and antitumor activities of chitosan from shiitake stipes, compared to commercial chitosan from crab shells. Carbohydrate Polymers, Vol 138 pp 259-264.

Crini G, Morin-Crini N, Fatin-Rouge N, et al. (2017). Metal removal from aqueous media by polymer-assisted ultrafiltration with chitosan. Arabian Journal of Chemistry, Vol 10 pp 3826-3839.

Ferreira SA, Castillo OS, Santana TM, et al. (2020). Production and physicochemical characterization of chitosan for the harvesting of wild microalgae consortia. Biotechnology Reports, Vol 28 pp e00554.

Gharieb MM, El-Sabbagh SM, Shalaby MA et al. (2015). Production of chitosan from different species of zygomycetes and its antimicrobial activity. International Journal of Engineering Research, Vol 6 No 4 pp 123-130.

Haj NQ, Mohammed MO and Mohammood LE (2020). Synthesis and Biological Evaluation of Three New Chitosan Schiff Base Derivatives. ACS Omega, Vol 5 No 23 pp 13948-13954.

Hamid AA, Aiyelaagbe OO, Ahmed RN, et al. (2011).

- Preliminary phytochemistry, Antibacterial and Antifungal Properties of extracts of *Asystasia gangetica* Linn T. Anderson grown in Nigeria. *Advances in Applied Science Research*, Vol 2 No 3 pp 219-226.
- Holappa J, Nevalainen T, Soininen P, et al. (2005). N-chloroacyl-6-O-triphenylmethylchitosans: Useful intermediates for synthetic modifications of chitosan. *Biomacromolecules*, Vol 6 No 2 pp 858-863.
- Hosseinejad M and Jafari SM (2017). Evaluation of different factors affecting antimicrobial properties of chitosan. *International Journal of Biological Macromolecules*, Vol 85 pp 467-475.
- Jauris IM, Matos CF, Zarbinb AJG, et al. (2017). Adsorption of anti-inflammatory nimesulide by graphene materials: a combined theoretical and experimental study. *Physical Chemistry Chemical Physics*, Vol 19 No 33 pp 22099-22110.
- Jiao TF, Zhou J, Zhou J, et al. (2011). Synthesis and Characterization of Chitosan-based Schiff Base Compounds with Aromatic Substituent Groups. *Iranian Polymer Journal*, Vol 20 No 2 pp 123-36.
- Kumari S, Annamareddy SHK, Abanti S et al. (2017). Physicochemical properties and characterization of chitosan synthesized from fish scales, crab and shrimp shells. *International Journal of Biological Macromolecules*, Vol 104 pp 1697-1705.
- Kundu T and Pramanik A (2020). Expedient and eco-friendly synthesis of new multifunctionalized pyrrole derivatives and evaluation of their antioxidant property. *Bioorganic Chemistry*, Vol 98 pp 103734.
- Lal S, Arora S, Rani S, et al. (2020). Synthesis and characterization of water-soluble chitosan derivatives: spectral, thermal and biological studies. *Journal of Macromolecular Science, Part A*, Vol 57 No 12 pp 791-799.
- Lallana E, Rosa JMRDL, Tirella A, et al. (2017). Chitosan/hyaluronic acid nanoparticles: rational design revisited for RNA delivery. *Molecular Pharmaceutics*, Vol 14 No 7 pp 2422-2436.
- Li J and Zhuang S (2020). Antibacterial activity of chitosan and its derivatives and their interaction mechanism with bacteria: Current state and perspectives. *European Polymer Journal*, Vol 138 pp 119984.
- Liu L, Yao W, Rao Y, et al. (2017). pH-Responsive carriers for oral drug delivery: challenges and opportunities of current platforms *Drug Delivery*, Vol 24 No 1 pp 569-581.
- Lo W, Deng F, Chang C et al. (2020). Synergistic Antifungal Activity of Chitosan with Fluconazole against *Candida albicans*, *Candida tropicalis*, and Fluconazole-Resistant Strains. *Molecules*, Vol 25 pp 5114.
- Ma G, Yang D, Zhou Y, et al. (2008). Preparation and characterization of water-soluble N-alkylated chitosan *Carbohydrate. Polymers*, Vol 74 No 1 pp 121-126.
- Mahira S, Jain A, Khan W et al. (2019). Chapter 1: Antimicrobial Materials—An Overview in *Antimicrobial Materials for Biomedical Applications*, pp 1-37.
- Masci D, Hind C, Islam MK, et al. (2019). Switching on the activity of 1,5-diaryl-pyrrole derivatives against drug-resistant ESKAPE bacteria: Structure-activity relationships and mode of action studies. *European Journal of Medicinal Chemistry*, Vol 178 pp 500-514.
- Mati-Baouche N, Elchinger PH, de Baynast H, et al. (2014). Chitosan as an adhesive. *European Polymer Journal*, Vol 60 pp 198-212.
- Mobarak NN and Abdullah MP (2010). Synthesis and characterization of several lauryl chitosan derivatives. *Malaysian Journal of Analytical Sciences*, Vol 14 No 2 pp 82-99.
- Nadia M, Eric L, Giangiaco T et al. (2019). Applications of chitosan in food, pharmaceuticals, medicine, cosmetics, agriculture, textiles, pulp and paper, biotechnology, and environmental chemistry. *Environmental Chemistry Letters*, Springer Verlag, Vol 17 No 4 pp 1667 – 1692.
- Pânzariu AT, Apotrosoaei M, Vasincu IM, et al. (2016). Synthesis and biological evaluation of new 1,3-thiazolidine-4-one derivatives of nitro-L-arginine methyl ester. *Chemistry Central Journal*, Vol 10 No 1 pp 6.
- Parmar K, Sutariya S, Shukla M et al. (2012). Synthesis and Antimicrobial Activity of Substituted 2H-pyrrole-2-ones Derivatives Based on 1-N-Phenyl-3-phenyl-4-formyl pyrazole (PFP). *Journal of Chemical and Pharmaceutical Research*, Vol 4 pp 3478-82.
- Pati S, Chatterji A, Dash BP, et al. (2020). Structural Characterization and Antioxidant Potential of Chitosan by γ -Irradiation from the Carapace of Horseshoe Crab. *Polymers*, Vol 12 pp 2361.
- Pragłowska JR, Piatkowski M, Dieneka V, et al. (2019). Chitosan-Based Bioactive Hemostatic Agents with Antibacterial Properties-Synthesis and Characterization. *Molecules*, Vol 24 No 14 pp 2629.
- Shang BB, Sha J, Liu Y, et al. (2011). Synthesis of a new chitosan derivative and assay of *Escherichia coli* adsorption. *Journal of Pharmaceutical Analysis*, Vol 1 No 1 pp 39-45.
- Verlee A, Mincke S and Stevens CV (2017). Recent developments in antibacterial and antifungal chitosan and its derivatives. *Carbohydrate Polymers*, Vol 164 pp 268-283.
- Wang H, Han X, Shi H, et al. (2014). Crystalline structure and phase behavior of N-alkylated polypyrrole comb-like polymers. *CrystEngComm*, Vol 16 pp 7090-7096.
- Wang P, Lv X, Zhang B, et al. (2021). Simultaneous determination of molar degree of substitution and its distribution fraction, degree of acetylation in hydroxypropyl chitosan by ^1H NMR spectroscopy. *Carbohydrate Polymers*, pp 117950.
- Xia W, Liu P, Zhang J et al. (2011). Biological activities of chitosan and chitooligosaccharides. *Food Hydrocolloids*, Vol 25 No 2 pp 170-179.